

Analytical Method for the Ditching Analysis of an Airborne Vehicle

Farhad Ghaffari*
ViGYAN, Inc., Hampton, Virginia

A simple analytical method has been introduced for aerohydrodynamic load analysis of an airborne configuration during water ditching. The method employs an aerodynamic panel code, based on linear potential flow theory, to simulate the flow of air and water around an aircraft configuration. The free surface separating the air and water region is represented by doublet singularities. Although all the theoretical load distributions are computed for air, provisions are made to correct the pressure coefficients obtained on the configuration-wetted surfaces to account for the water density. As an analytical tool, a vortex aerodynamic code is chosen to carry out the present investigation. After assessing the validity of the method, an application is presented for the water ditching of the Space Shuttle configuration at a 12-deg attitude.

Nomenclature

C_p	= pressure coefficient, $(p - p_\infty)/q_\infty$
c	= chord, in.
ℓ	= wetted-chord length with wave rise model, in.
ℓ'	= wetted-chord length without wave rise model, in.
M	= Mach number
V	= total velocity, ft/s
q	= dynamic pressure, psi
X, Y, Z	= global coordinate system
X/ℓ	= fractional distance along the local wetted chord
α	= angle of attack, deg
β	= trailing wake deflection angle, deg
η	= fraction of wing theoretical semispan
ρ	= density, slug/ft ³

Subscripts

a	= air
r	= root
w	= water
∞	= freestream

Introduction

VARIOUS malfunctions, such as engine power failure, can cause an emergency ditching for an aircraft while operating over water. Although aircraft ditching does not frequently occur, a number of experimental studies have been performed¹⁻⁴ with a common objective that is mainly directed at understanding the ditching process and the subsequent hydrodynamic loads. The results from these investigations allow the designers of an aerospace vehicle to make reasonable initial judgments on the design parameters, such as the selection of the material and/or structural arrangement that minimize the impairment resulting from the water loads. It is often possible to incorporate additional design features that will give some measure of ditching safety with minimum penalties to the aerodynamic properties of the aircraft.

Most aircraft water ditching studies have been experimental

using dynamically scaled models or full-scaled vehicles. Although these past studies provide qualitative assessments on the effects of the resulting hydrodynamic loads and overall impact on the model, no quantitative information on the problem can be extracted. The purpose of the present study is to evaluate an analytical method capable of simulating the aerohydrodynamic flowfield around an aircraft during water ditching. The method is based on linear potential flow theory, employing lower order panels for aerodynamic surfaces and doublet sheet singularities to model the free surface at the air-water interface. This doublet sheet separates the incoming flow into upper and lower part flow regions. The computed loads, obtained on the configuration surfaces interacting with lower part flow region, are subsequently corrected to account for the density differences between air and water. Furthermore, appropriate provisions have been made to model the trailing wake system associated with a ditching configuration.

This analytical method for water ditching was primarily developed for its application to the Space Shuttle configuration. As discussed in Ref. 5, the ascent phase of the Space Shuttle flight profile starts with ignition of the solid rocket boosters and finishes at orbit insertion. In the case of a mis-

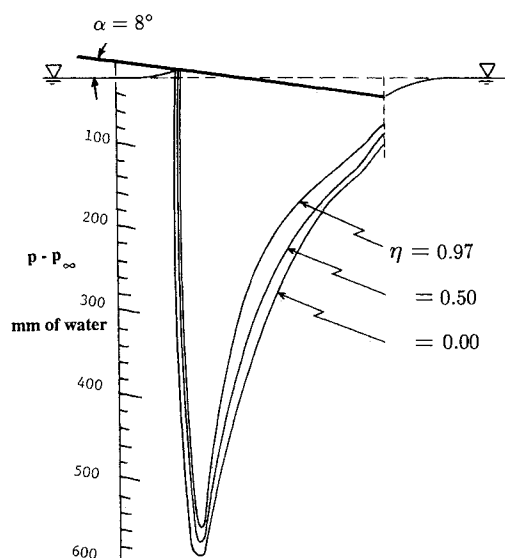


Fig. 1 Experimental hydrodynamic pressure distribution on a flat rectangular plate at $\alpha = 8$ -deg, $V_\infty = 19.7$ ft/s.

Presented as Paper 88-2521 at the AIAA 6th Applied Aerodynamics Conference, Williamsburg, VA, June 6-8, 1988; received April 29, 1989; revision received Oct. 26, 1989. Copyright © 1988 American Institute of Aeronautics and Astronautics, Inc. All rights reserved.

*Research Engineer. Senior Member AIAA.

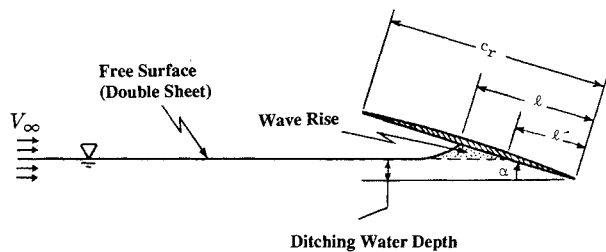


Fig. 2 Cross section of a flat-bottom, rectangular plate during water ditching.

sion abort in the ascent phase, the orbiter is required to release the solid rocket boosters and the external fuel tank and then return to the launch site. However, if the orbiter is unable to return to the ground airfield facility, an alternative is to land the vehicle in the ocean. Hence, it is essential to understand the process of ditching including its hydrodynamic effects on the vehicle.

No experimental data are available on the ditching of the Space Shuttle orbiter to make any direct hydrodynamic load comparison between the data and the theoretical results. However, efforts have been made to assess the validity of the present analytical ditching method. This validation effort includes a comparison between the theoretical prediction and the experimental hydrodynamic load data acquired on a flat rectangular plate during water ditching. A more detailed discussion of the results from this study has been presented in Ref. 6.

The theoretical results presented are obtained by employing an aerodynamic panel code called Vortex Separation Aerodynamics (VSAERO).⁷ The code is based on the solution to the Laplace equation about an arbitrary three-dimensional configuration. Source and doublet singularities are distributed in a piecewise constant fashion on each quadrilateral surface panel. The unknown singularity strengths are determined by imposing the external Neumann and internal Dirichlet boundary conditions on each panel.

Ditching Method and Evaluation

It is essential to assess the validity of the analytical ditching method developed in the present study. As a result, a literature survey was conducted to retrieve experimental data for the ditching of a geometrically simple configuration. The survey led to the hydrodynamic load data reported by Sottorf.⁸ Sottorf's experiments on ditching were conducted in a towing tank on different flat plates at various flow conditions. A set of plots have been selected from his report to provide the baseline experimental data for comparative assessments with the computational results obtained from the present analytical ditching method. The data (see Fig. 1) show the measured chordwise pressure distribution for a simple rectangular plate at an 8-deg angle of attack and 19.7 ft/s (i.e., 6 m/s) towing speed.

Test-Case Configuration

The computational, test-case configuration is defined by a rectangular plate having an aspect ratio of 2.33, a circular-arc section (thickness ratio of 1.7% with maximum occurring at midchord), and a flat lower surface. The configuration is pitched up about the trailing edge and set at an 8-deg angle of attack, which corresponds to the experimental hydrodynamic data. The complete configuration is represented using 391 surface panels.

Free-Surface Modeling

The free surface of the water is represented by doublet sheet singularities with an imposed no flow through boundary condition. This flat surface, situated at zero angle of attack with respect to the freestream, begins at its intersection with the

lower surface of the ditching configuration and is extended upstream to about three times the configuration root chord (see Fig. 2). The free surface can be envisioned as a dividing stream surface that separates the incoming flow into two parts: the upper surface air region and the lower surface water region. Although theoretically, both regions are exposed to air flow, the aerodynamic loads computed for the lower surface wetted region are then corrected, in postprocessing, to account for the water density.

It is important to note that the present method for modeling the free surface is an approximation to a more advanced approach, which among other factors includes the effects of wave resistance. Boppe et al.⁹ presented an excellent discussion on the complexity involved in using the latter approach to design the 12-m yacht "Stars and Stripes '87." Since the free-surface distortion is not allowed in the present method, a study is performed to investigate the effects of wave rise (see Fig. 2) on the surface load distribution. As discussed in Ref. 10, the wave rise occurs in front of a flat-bottom plate during planning. This wave rise causes the running wetted length (ℓ) to be larger than the length (ℓ') defined by the undisturbed water level intersection with bottom surface of the plate. As expected, this study revealed that the volume of the wave rise region can be altered by changing the ratio of ℓ/ℓ' . Furthermore, any increase in the wave rise volume causes a flow deceleration in the region. This flow retardation results in an increase in the positive pressure peak in the vicinity of the wave-rise cavity region. It is difficult to justify any specific value for the ℓ/ℓ' ratio because it depends on many variables such as the configuration geometry, angle of attack, depth of water (measured vertically from the configuration trailing edge to the free surface), and ditching speed, and it is time dependent. However, this ratio is given in Sottorf's report for the flat rectangular plate that was tested at steady state in a towing tank. As a result, this ratio was used to determine the length ℓ for a given length ℓ' , which is known when a water ditching depth is selected. Furthermore, a smooth curve was used to define the shape of the free-surface curvature just before intersecting the lower surface of the ditching configuration. A similar procedure was used to model the wave-rise region for the Shuttle ditching application. It should be noted that the approximations used in the present method of modeling the free surface ignore the important time dependent effects of the wave-dynamic motions during water ditching.

Trailing Wake Modeling

Three approaches were studied to model the trailing-wake system of the test case configuration during water ditching. The various steady, planar wake models studied are shown in Fig. 3. As seen from the figure, the first approach does not allow a change to occur in the vertical height level of the wake as it leaves the configuration trailing edge. The second approach allows the trailing wake system to vary linearly starting at the trailing edge and terminating downstream at the free-surface atmospheric level where it becomes constant. The

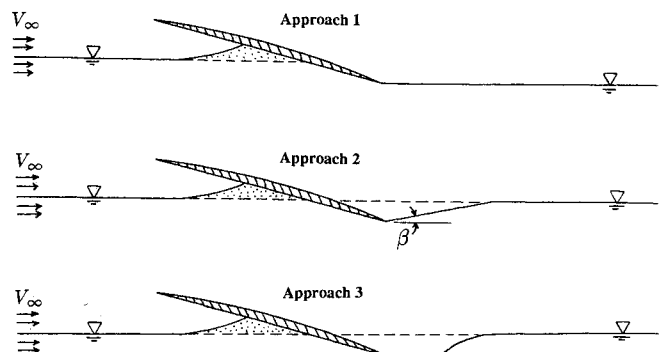


Fig. 3 Trailing wake models of a flat-bottom, rectangular plate during ditching.

angle at which the wake lines leave the trailing edge is chosen to be twice the configuration angle of attack (i.e., $\beta = 16$ -deg, see Fig. 3). The third approach defines the trailing-wake system by a curve path rather than a linear connection. This curved-wake system leaves the trailing edge tangent to the configuration lower surface and blends smoothly into the free-surface atmospheric level downstream.

The computed results on the test-case configuration utilizing the wake system defined in the third approach will be shown later. However, it was found that the effects of different aforementioned trailing-wake modeling on the computed aerodynamic load distributions were small. Hence, for the purpose of simplicity, it was decided to select the trailing-wake system defined in the first approach to be used in the ditching application to the Shuttle configuration.

Density Correction

The pressure coefficient is defined as:

$$C_p = \frac{p - p_\infty}{\frac{1}{2}\rho_\infty V_\infty^2} = \frac{p - p_\infty}{q_\infty} \quad (1)$$

where ρ_∞ , V_∞ , and q_∞ are the freestream fluid density, velocity, and dynamic pressure, respectively. According to incompressible potential flow theory, the fluid density is assumed to be constant. As a result, the term ρ_∞ in the above equation can be interpreted as a scaling factor, which remains constant for a given fluid media. For example, the constant density assumption allows the aerodynamic pressure coefficients computed on a configuration to be converted to hydrodynamic loads by a simple multiplication factor determined by the ratio of air-to-water density. Hence, Eq. (1) becomes

for air

$$C_p = \frac{p - p_\infty}{\frac{1}{2}\rho_{\infty,a} V_\infty^2} = \frac{p - p_\infty}{q_{\infty,a}} \quad (2)$$

and for water

$$C_p = \frac{p - p_\infty}{\frac{1}{2}\rho_{\infty,a} V_\infty^2} \frac{\rho_{\infty,a}}{\rho_{\infty,w}} = \frac{p - p_\infty}{q_{\infty,w}} \quad (3)$$

where the subscripts a and w denote the air and water properties, respectively.

The experimental hydrodynamic load distributions for the test-case configuration have been reported⁸ as a pressure dif-

ference between the local and atmospheric level (i.e., $p - p_\infty$) expressed in mm of water. To be consistent, the computed loads are converted to that of the experimental form. It follows from Eqs. (2) and (3) that

$$p - p_\infty = C_p q_{\infty,a} \quad (4)$$

$$p - p_\infty = C_p q_{\infty,w} \quad (5)$$

Furthermore, the selected experimental data on the test-case configuration were obtained for an 8-deg angle of attack and freestream of 19.7 ft/s. As a result, the corresponding air and water dynamic pressures are given by

$$\begin{aligned} q_{\infty,a} &= \frac{1}{2}\rho_{\infty,a} V_\infty^2 \\ &= \frac{1}{2}(0.00237 \text{ slug/ft}^3)(19.7 \text{ ft/s})^2 \text{ ft}^2/144 \text{ in.}^2 \\ &= 0.00319 \text{ psi} \equiv 2.25 \text{ mm of water} \\ q_{\infty,w} &= \frac{1}{2}\rho_{\infty,w} V_\infty^2 \\ &= \frac{1}{2}(1.94 \text{ slug/ft}^3)(19.7 \text{ ft/s})^2 \text{ ft}^2/144 \text{ in.}^2 \\ &= 2.61 \text{ psi} \equiv 1839.57 \text{ mm of water} \end{aligned}$$

These values of the dynamic pressures for air and water are coupled with the computed aerodynamic pressure coefficients in Eqs. (4) and (5) to determine the aerohydrodynamic load distribution on the ditching configuration.

Results and Discussions

The VSAERO computer code is applied to the test-case configuration to evaluate the validity of the present analytical ditching method. An isometric view of the surface panels representing the ditching configuration set at an 8-deg angle of attack, the trailing-wake system, and the modeled free surface are shown in Fig. 4. A typical chordwise pressure coefficient computed on the test-case configuration along with the corresponding geometry sectional cut are plotted in Fig. 5. In addition, the figure shows the pressure coefficients on the free-surface panels that are situated just ahead of the ditching configuration. The pressure coefficients and the total velocity magnitudes, computed on the free-surface panels upstream of those shown in the figure, approach those of the freestream flow conditions.

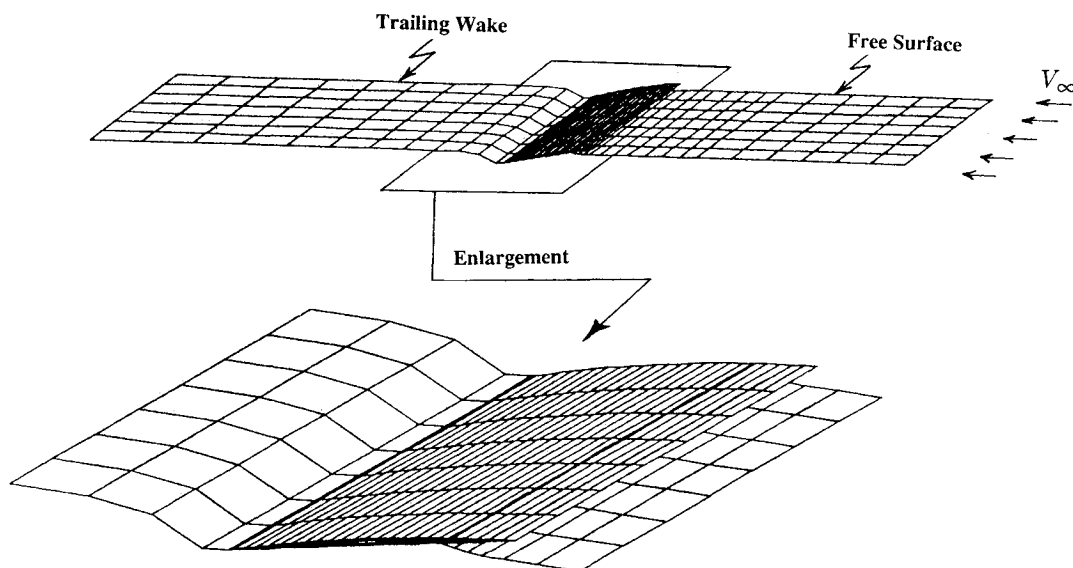


Fig. 4 Surface panel representation of the test-case configuration at 8-deg angle of attack.

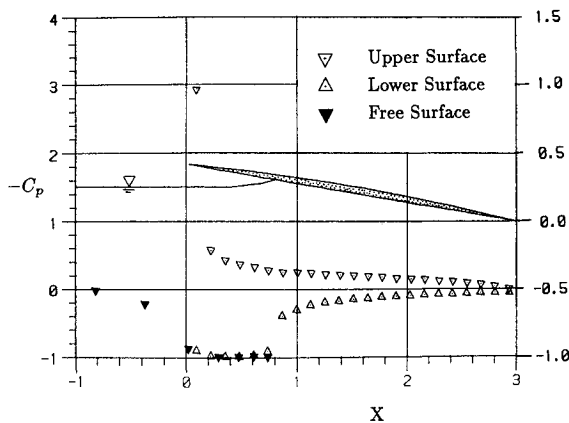


Fig. 5 Computed chordwise pressure distribution on the test-case configuration in free air at $\alpha = 8$ deg, $M_\infty = 0$, $\eta = 0.50$.

The solutions shown in Fig. 5 are all computed for free air and have not been corrected to account for the water density. It is evident from the figure that the computed upper surface pressure distributions are not affected by the ditching process. However, as expected, ditching has significant effects on the lower surface pressure distributions. The configuration lower surface experiences two distinct flow characteristics, which are separated by the presence of the free surface. The flow passing above the free surface is trapped in the cavity region, and the flow passing under the free surface proceeds toward the configuration trailing edge. It can be seen from Fig. 5 that the reduced velocity magnitude (approximately zero) in the cavity region results in a compressed flow, which drives the computed pressure coefficients toward unity. However, the flow passing under the free surface is mildly expanded on the lower surface of the ditching configuration, which reduces the pressure coefficients to about zero at the trailing edge. The lower surface panels that are aft of the free-surface intersection with the configuration are considered to be exposed to water. Consequently, the pressure coefficients computed on the wetted panels are corrected to account for the change in the density.

The hydrodynamic load distribution on the wetted panels have been obtained from the computed pressure coefficients using Eq. (5) and are plotted in Fig. 6. For comparison purposes, this figure also shows the experimental data for a flat rectangular plate reported by Sottorf.⁸ It should be noted that the theoretical solution computed at the inboard ($\eta = 0.07$) and outboard ($\eta = 0.93$) span stations are slightly different from those of the experimental locations because the theoretical solutions are computed at the center point of each panel rather than at the edges. The figure shows that the overall comparison between computational results and the experimental data are generally good. To be more explicit, one can confine the existing disagreements to three main regions. These are the trailing edge, the tip, and the wave-rise region where the maximum positive pressure occurs. It appears that the theoretical results can be manipulated to compel an even better comparison with the data by simply modifying the trailing-wake system, wave-rise region, and/or extending/shaping of the free surface outboard of the tip region. However, since the water surface characteristics for the test-case configuration are not known in these regions, no attempts were made to further modify the original free-surface modeling.

Space Shuttle Analysis

The preliminary application of the VSAERO computer code to the Space Shuttle water ditching is discussed in three parts. The first part is a discussion on the Space Shuttle geometry preparation. The second part addresses the validity of the computed results on the Shuttle configuration in free air. This validation effort is established through a comparison between the computed pressure coefficients and the available experi-

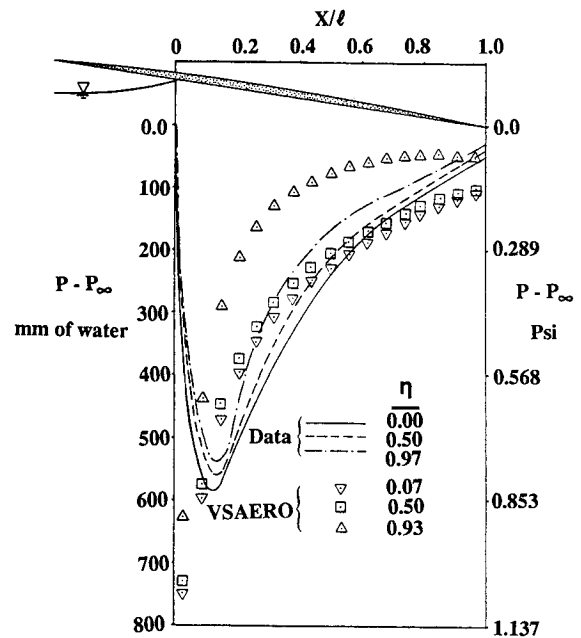


Fig. 6 Computational and experimental hydrodynamic chordwise pressure distribution for a rectangular plate, $\alpha = 8$ deg, $V_\infty = 19.7$ ft/s.

mental wind-tunnel data. The third part of the study includes an investigation on the computational results that are obtained on the Shuttle configuration for three different altitudes with respect to the free surface. The three different altitudes are designed to simulate the flow around the orbiter in free air, the vicinity of the water surface, and water ditching.

Geometry Preparation

The geometry preparation often plays an important part of any computational analysis especially when lower order (constant source and doublet singularity distributions) surface panel aerodynamic codes such as VSAERO are being utilized. For such computer codes, fine surface-panel resolution on the aircraft configuration is required for an accurate computational result. However, the 1000-panel version of the VSAERO code limited the maximum number of surface panels that could be used in the present study. As a result, a single arrangement for the surface-panel distribution was generated for the complete Shuttle configuration that could be used in the proceeding analysis without any further modification. The analysis include both the free-air evaluation of the VSAERO results against the experimental data and the Shuttle-ditching application with free-surface modeling. It should be noted that all the geometry manipulations such as surface paneling rearrangement, determination of the free-surface intersection with the Shuttle configuration, etc., are performed interactively using a computer code called GEOMX.¹¹ Moreover, all the dimensions reported on the Shuttle configuration are taken from a full-scale vehicle.

An angle of attack of 12-deg and zero Mach number are chosen as the flow conditions used for the Shuttle ditching analysis. Furthermore, the water-ditching depth (height measured vertically from the Shuttle configuration minimum point to the free surface) of 98.3 in. is selected to provide the height level of the free-surface relative to the configuration. The selected water-ditching depth is about 0.1 of the wing root chord. As the first step, the intersection of the free surface with the configuration is required for any future paneling rearrangements. The Shuttle configuration with its original surface panels is initially pitched up to the desired 12-deg angle of attack. A horizontal cut through the complete configuration is made at the given height level selected for the free surface. Figure 7 shows the side and the front view of the

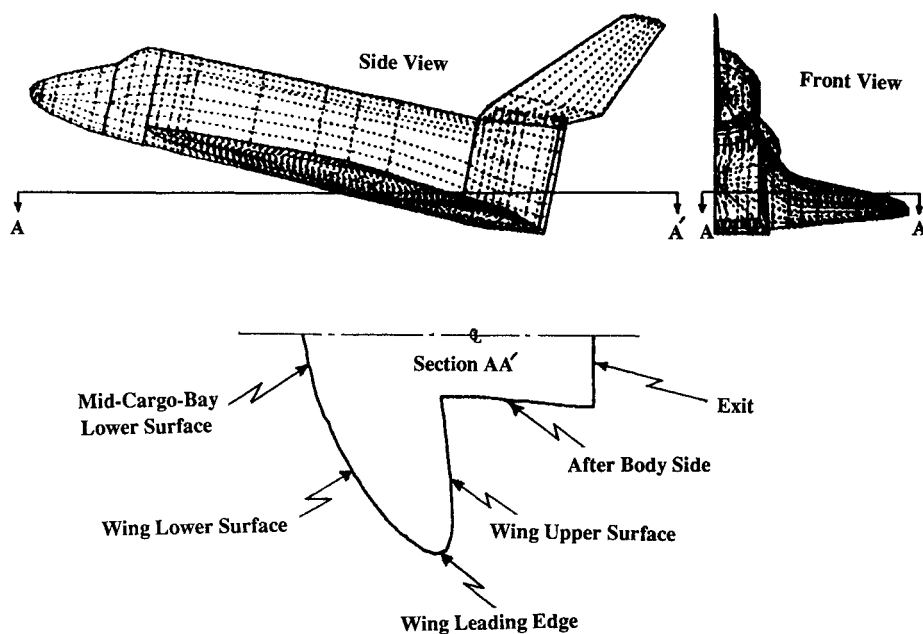


Fig. 7 Sectional cut through the Shuttle configuration at the free surface height level.

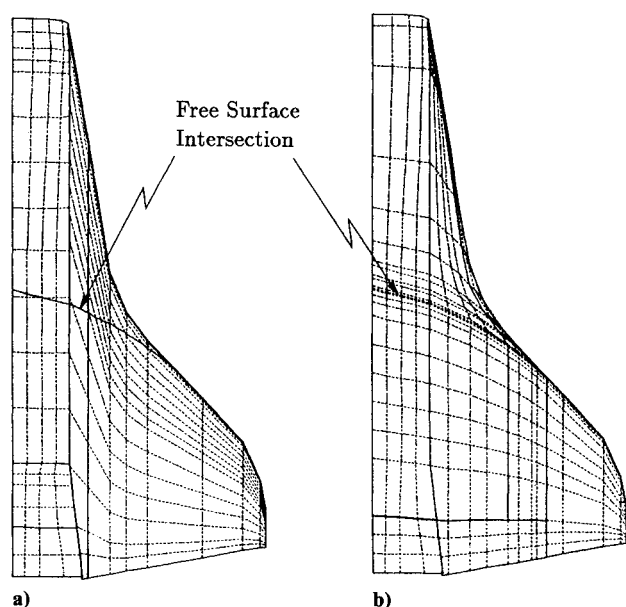


Fig. 8 Free surface intersection with windward side of the Shuttle configuration; a) original panels, and b) modified panels.

Shuttle configuration with a conventional paneling arrangement. This figure also shows the location of the cut as well as the resulting intersection contour.

A more informative view of the free-surface intersection with the windward side of the Shuttle configuration is shown in Fig. 8a. The lower surface panels on the wing as well as the cargo bay are modified around the free-surface intersection line. As shown in Fig. 8b, this modification on the windward side of the configuration is necessary to separate the wetted panels exposed to the water from those exposed to the air flow. Moreover, this new arrangement provides an improved panel resolution and also allows for an exact abutment between the surface panel edges of the free surface and the Shuttle lower surface. The total number of panels on the modified Shuttle geometry is 841, excluding the vertical tail. The vertical tail has been neglected because its presence should have minimal aerodynamic effects on the present study.

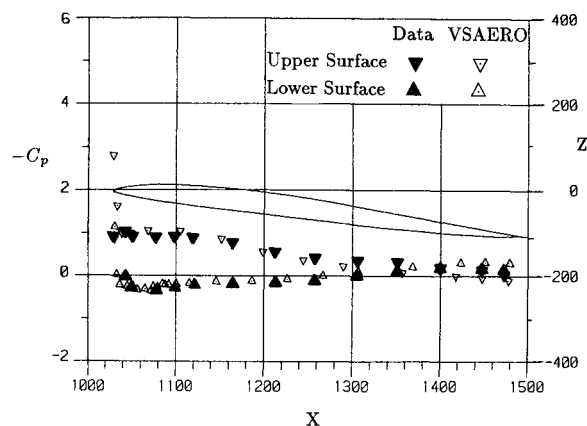


Fig. 9 Computational and experimental chordwise pressure distribution on the Shuttle configuration in free air at $\alpha = 12.5$ -deg, $M_\infty = 0.60$, $\eta = 0.43$.

Now that the free-surface intersection line with the windward side of the Shuttle configuration is determined, the construction of the free-surface model only depends on a dimension that defines its upstream extent. Consequently, it appeared sufficient to extend the free-surface model to about 1000 in. (slightly larger than the wing-root chord) upstream. Furthermore, a procedure similar to the one used for the test-case configuration was employed to incorporate the wave-rise curvature to the flat free surface just before its intersection with the Shuttle configuration. It is important to note that the spanwise extent of the free surface, outboard of its intersection with the wing leading edge, is not modeled in the present study. This decision is made because of the difficulty in predicting an appropriate shape for the free-surface model above the submerged wing-tip region. This region, located under the free-surface cutting plane, is clearly shown in the front view of the Shuttle configuration in Fig. 7. The absence of the free surface in the tip region would allow the spanwise flow that is growing above and below the modeled free surface inboard of the submerged tip region to split at the wing leading edge with no geometrical constraints.

Free Air Evaluation

This part of the study evaluates the applicability of the VSAERO code to the Space Shuttle configuration in free air. This evaluation is verified through a direct comparison between the computed pressure coefficients and the available experimental wind tunnel data at 12.5-deg angle of attack and 0.6 Mach number. The experimental data¹² are obtained on a 0.03-scale model tested in the NASA Ames Research Center unitary plan wind tunnels.

The computed chordwise pressure distribution at a typical wing semispan location is shown in Fig. 9. This figure also shows the experimental wind-tunnel data as well as the wing cross-sectional geometry for the same semispan location. The horizontal and vertical axis represent the full-scale coordinates of the Shuttle configuration. The computed pressures compare very well with the available data at this station as well as other wing semispan locations.⁶ It should be noted that the crossing of the experimental upper and lower surface pressure distribution near the wing trailing edge is well predicted by the theory across the span.

Ditching Application

As part of the analytical ditching application to the Space Shuttle configuration, it is instructive to include the corresponding free-air and ground-effect calculations. A total of three cases are examined, at 12-deg angle of attack and Mach number of zero with various altitude with respect to the water surface. These altitudes are designed to simulate the flow conditions around the Shuttle configuration in 1) free air, 2) vicinity of water, and 3) water ditching. Side-view panel representations of the orbiter operating at these altitudes are shown in Fig. 10. This figure also shows the truncated trailing-wake models associated with each case. Furthermore, two isometric views of the Shuttle configuration with the modeled free surface are shown in Fig. 11. The geometry on the top clearly illustrates the outboard extent of the free surface with respect to the wing span and its position along the leading edge. Moreover, the geometry shown on the bottom part of the figure illustrates the surface panel arrangements on the free surface and the wetted region on the Shuttle configuration.

The computed pressure coefficients on the Shuttle configuration are shown in Fig. 12 for various cases studied. The figure also shows the corresponding streamwise sectional cut through the modeled configuration. The VASERO code has a built-in feature for ground effect analysis, which allows a user to specify the X - Y plane at zero elevation (i.e., $Z = 0$) to represent the ground. Hence, the surface panel coordinates associated with a configuration are required to be transferred

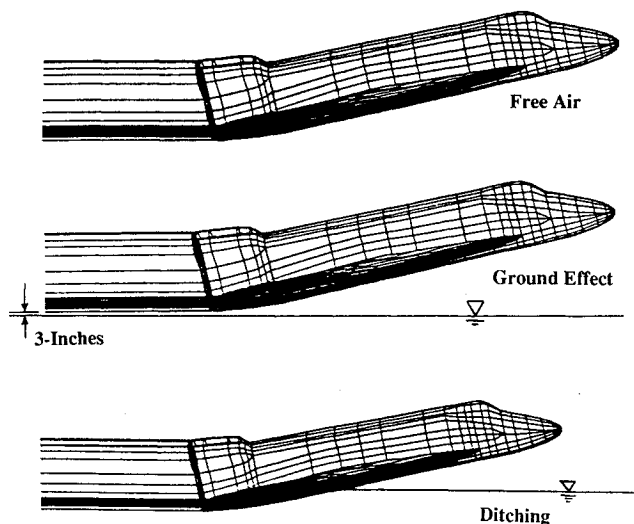


Fig. 10 Side view illustration of the Shuttle configuration in free air, ground vicinity, and ditching.

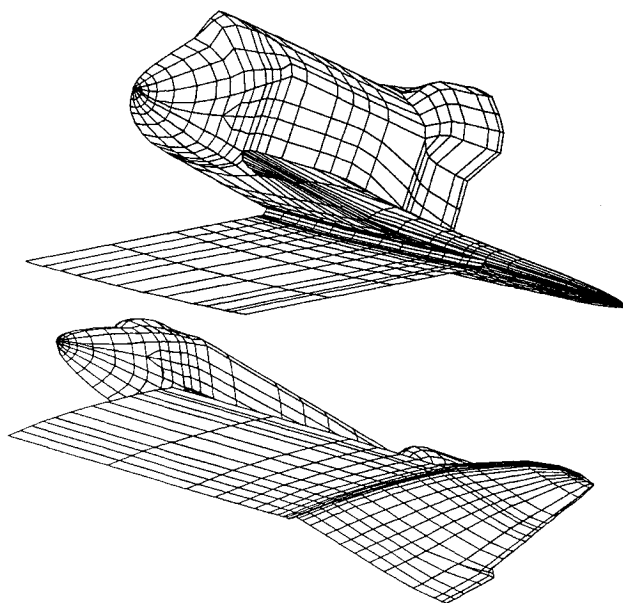


Fig. 11 Two isometric views of the surface panels on the Shuttle configuration with modeled free surface.

up above the X - Y plane according to the desired ground height elevation. As a result, the Z coordinates associated with the streamwise sectional cut shown for ground effect in Fig. 12 are different from those of the free air and/or ditching. Furthermore, the pressure coefficients that are shown in the figure are all computed for air.

It is evident from the distribution of the computed pressure coefficients that the presence of the ground results in the upper-surface flow expansion especially in the outboard region and the lower-surface flow compression particularly in the inboard region, as expected. It appears that the ditching operation has minimal effects on the configuration upper-surface pressure distributions with the exception of the flow expansion around the leading-edge portion of the wing section where the outboard tip of the free surface is located. This expansion is largely due to the growth of the spanwise flow in the cavity region between the free surface and the lower surface of the Shuttle configuration. The pressure distribution on the fuselage of the Shuttle configuration during ditching (bottom of Fig. 12a) reveals two clear stagnation points (i.e., $V \approx 0$, $C_p \approx 1$) at a span station positioned approximately along the configuration plane of symmetry. The first one is located on the lower surface of the forebody and the second one is at the free-surface intersection with the configuration lower surface. There is no evidence of these stagnation points occurring outboard of this station because the magnitude of the sidewash velocity component increases in the spanwise direction.

The presence of the free surface causes the lower surface of the Shuttle configuration to experience two distinct flow characteristics (see Fig. 12): the upper free-surface flow, which is trapped in the cavity region, and the lower free surface flow, which proceeds toward the configuration trailing edge. The retarded air flow in the cavity region results in approximately the same pressure distribution on the configuration lower surface as on the free surface. Upstream of the cavity region, the pressures on the free surface approach those of the freestream conditions. The lower free-surface flow starts to expand once passed downstream of the waterline intersection with the Shuttle lower surface, thereby, reducing the neighboring surface pressure coefficients.

As previously discussed, the only parameter needed for the conversion of the computed aerodynamic properties to those of hydrodynamic is the dynamic pressure. The dynamic pressure is readily determined from landing speed of the ditching

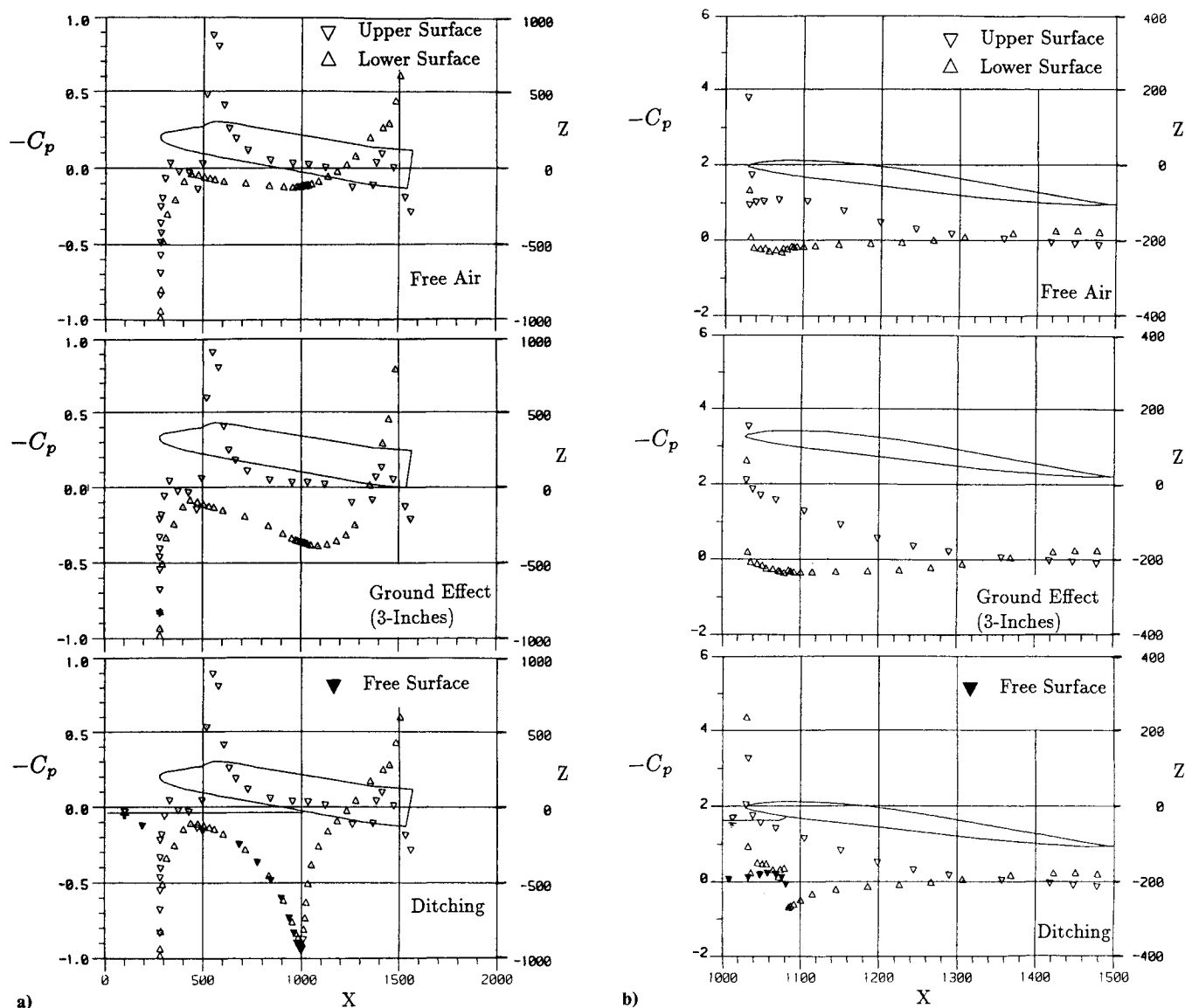


Fig. 12 Computed streamwise pressure distribution on the Shuttle configuration in free air, ground vicinity, and ditching, $\alpha = 12$ deg, $M_\infty = 0$; a) $\eta = 0.004$, and b) $\eta = 0.43$.

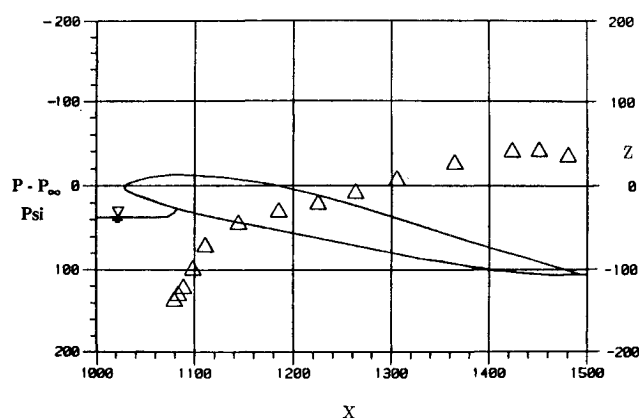


Fig. 13 Computed chordwise hydrodynamic load distribution on the Shuttle's wing at $\alpha = 12$ deg, $V_\infty = 100$ knots, $\eta = 0.43$.

configuration. For example, two steps are required to compute the hydrodynamic pressure distribution on the wetted panels of the Shuttle configuration having a ditching speed of 100 knots (i.e., 168.78 ft/s). The first step is to find $q_{\infty, w}$ as follows

$$\begin{aligned} q_{\infty, w} &= \frac{1}{2} \rho_{\infty, w} V_\infty^2 \\ &= \frac{1}{2} (1.94 \text{ slug/ft}^3) (168.78 \text{ ft/s})^2 \text{ ft}^2 / 144 \text{ in.}^2 \\ &= 191.9 \text{ psi} \end{aligned}$$

The second step is to multiply the above value by all the aerodynamic pressure coefficients computed on the wetted panels. Figure 13 illustrates an example of the resulting hydrodynamic load distribution obtained for the wing section at $\eta = 0.43$ with ditching speed of 100 knots. The results shown in this figure have been obtained by rescaling the aerodynamic pressure coefficients computed on the wetted panels, which were depicted earlier in the bottom of Fig. 12b.

Concluding Remarks

The present study demonstrated the applicability of a simple method developed for aerohydrodynamic load analysis of an

airborne vehicle during water ditching. The method employs an aerodynamic panel code, based on linear potential flow theory, to simulate the flow of air and water around the ditching configuration. A doublet sheet is used to represent the free surface.

The validity of the method was first examined using the available experimental hydrodynamic load data for a rectangular plate configuration. A reasonable comparison between the computational results and experimental data was achieved. The method was then applied to analyze the ditching effects on the Space Shuttle configuration. The computed aerodynamic pressure coefficients on the Shuttle configuration with modeled free surface are reported along with a sample calculation for their conversion to the corresponding hydrodynamic load data in the wetted region.

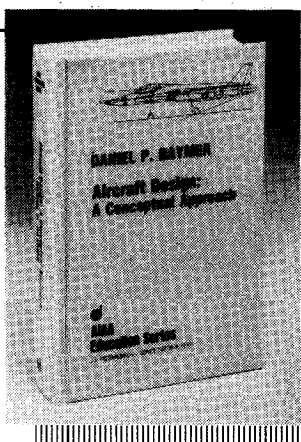
Finally, for future investigations, it is recommended that the accuracy of the present simple analytical method be examined against a more advanced free surface modeling that includes the effects of wave resistance, time dependency of wave motions, vehicle dynamics, and viscosity.

Acknowledgments

This work was sponsored by NASA Langley Research Center under Contract NAS1-18585.

References

- ¹Thomas, W. L., "Ditching Investigation of a 1/20-scale Model of the Space Shuttle Orbiter," NASA CR-2593, Oct. 1975.
- ²Fisher, L. J., and Hoffman, E. L., "Ditching Investigations of Dynamic Models and Effects of Design Parameters on Ditching Characteristics," NACA Rpt. 1347, 1958.
- ³McBride, E. E., "Preliminary Investigation of the Effects of External Wing Fuel Tanks on Ditching Behavior of a Sweptback Wing Airplane," NACA TN-3710, 1956.
- ⁴McBride, E. E., and Fisher, L. J., "Experimental Investigation of the Effect of Rear Fuselage Shape on Ditching Behavior," NACA TN-2929, 1953.
- ⁵McSwain, G., "Shuttle Ascent GN&C Postflight Results, Shuttle Performance: Lessons Learned," NASA CP-2283, Part 1, March 1983, pp. 581-594.
- ⁶Ghaffari, F., "An Analytical Method for Ditching Analysis of an Airborne Vehicle," NASA CR-4120, Feb. 1988.
- ⁷Maskew, B., "A Computer Program for Calculating the Nonlinear Aerodynamic Characteristics for Arbitrary Configurations," NASA CR-166476, Dec. 1982.
- ⁸Sottorf, W., "Experiments with Planing Surfaces," NACA TM-6611, Mar. 1932.
- ⁹Boppe, C. W., Rosen, B. S., Laiosa, J. P., and Chance, B., "Stars & Strips '87, Computational Flow Simulations for Hydrodynamic Design," Eighth Chesapeake Sailing Yacht Symposium, Annapolis, MD, March 1987.
- ¹⁰Savitsky, D., "Hydrodynamic Design of Planing Hulls," *Marine Technology*, Vol. 1, No. 1, Oct. 1964, pp. 71-95.
- ¹¹Hall, J. F., Neuhart, D. H., and Walkley, K. B., "An Interactive Program for Manipulation and Display of Panel Method Geometry," NASA CR-166098, March 1983.
- ¹²Chee, E., and Marroquin, J., "Results of Test Using a 0.030-Scale Pressure Loads Space Shuttle Orbiter Model (47-0) in the NASA/ARC Unitary Plan Wind Tunnels (OA149A)," NASA CR-151780, Vol. 2, Dec. 1979.



Aircraft Design: A Conceptual Approach

by Daniel P. Raymer

The first design textbook written to fully expose the advanced student and young engineer to all aspects of aircraft conceptual design as it is actually performed in industry. This book is aimed at those who will design new aircraft concepts and analyze them for performance and sizing.

The reader is exposed to design tasks in the order in which they normally occur during a design project. Equal treatment is given to design layout and design analysis concepts. Two complete examples are included to illustrate design methods: a homebuilt aerobatic design and an advanced single-engine fighter.

To Order, Write, Phone, or FAX:



Order Department

American Institute of Aeronautics and Astronautics
370 L'Enfant Promenade, S.W. ■ Washington, DC 20024-2518
Phone: (202) 646-7444 ■ FAX: (202) 646-7508

AIAA Education Series
1989 729pp. Hardback
ISBN 0-930403-51-7

AIAA Members \$46.95
Nonmembers \$56.95
Order Number: 51-7

Postage and handling \$4.75 for 1-4 books (call for rates for higher quantities). Sales tax: CA residents add 7%, DC residents add 6%. Orders under \$50 must be prepaid. Foreign orders must be prepaid. Please allow 4 weeks for delivery. Prices are subject to change without notice.